Network: Comput. Neural Syst. 9 (1998) 333–344. Printed in the UK PII: S0954-898X(98)93588-6

Irregular synchronous activity in stochastically-coupled networks of integrate-and-fire neurons

Juan K Lin†, Klaus Pawelzik‡, Udo Ernst‡ and Terrence J Sejnowski§

† Center for Biological and Computational Learning, Department of Brain and Cognitive Sciences, Massachusetts Institute of Technology, Boston, MA 02139, USA

‡ Max-Planck-Institute for Fluid Dynamics, and SFB 185 Nonlinear Dynamics, D-37018 Göttingen, Germany

§ Howard Hughes Medical Institute, Computational Neurobiology Laboratory, The Salk Institute, La Jolla, CA 92037, USA

Received 10 June 1997

Abstract. We investigate the spatial and temporal aspects of firing patterns in a network of integrate-and-fire neurons arranged in a one-dimensional ring topology. The coupling is stochastic and shaped like a Mexican hat with local excitation and lateral inhibition. With perfect precision in the couplings, the attractors of activity in the network occur at every position in the ring. Inhomogeneities in the coupling break the translational invariance of localized attractors and lead to synchronization within highly active as well as weakly active clusters. The interspike interval variability is high, consistent with recent observations of spike time distributions in visual cortex. The robustness of our results is demonstrated with more realistic simulations on a network of McGregor neurons which model conductance changes and after-hyperpolarization potassium currents.

1. Introduction

The significance of spike timing in cortical processing has been the focus of much current research. Mainen and Sejnowski (1995) showed that the firing times of neocortical neurons in slice preparations are highly reproducible when the same fluctuating stimulus is repeatedly injected. In cat visual cortex, Gray *et al* (1989) and Engel *et al* (1992) presented evidence for synchronization of action potentials between neighbouring cells. Softky and Koch (1993) reported high variability of the interspike intervals in their analysis of data from cat and macaque V1 and MT neurons, and argued that it is inconsistent with mean field temporal integration models where fluctuations are smoothed out.

In the present study, spatial and temporal aspects of firing patterns in a simple network model of integrate-and-fire neurons is examined in the context of rate coding and temporal coding. The coupling between neurons is stochastic as in Tsodyks and Sejnowski (1995b) and has a spatial structure that leads to clustering of localized attractors. Here we probe the strong coupling or small firing reset parameter regime (compare Vreeswijk and Sompolinsky (1996) and Troyer and Miller (1997)).

0954-898X/98/030333+12$19.50

2. Methods

The simplest single population time coarse-grained, mean-field model has dynamics given by

$$\dot{e}_i = -\alpha e_i + \sigma\left(\sum_j J_{ij} e_j + s_i - \theta\right) \tag{1}$$

where e_i represents the firing rate of neuron i, α is the decay time constant, $\sigma(\cdot)$ is a non-linear sigmoidal function such as $\tanh(\cdot)$, J_{ij} is the coupling matrix, s_i is the external stimulus and θ is the threshold term. Since the description is in terms of firing rates, detailed temporal aspects of the neuronal spiking activity are not captured. More descriptive models must be used to investigate the relevance of spike timing in cortical processing.

2.1. Network of integrate-and-fire neurons

The central model studied consists of a single population of integrate-and-fire neurons with both excitatory and inhibitory interactions. Time evolution of the network is given by

$$\tau \dot{V}_i = -(V_i - V_0) + \sum_j J_{ij} k_{ij}(t) \delta(t - t_j^{\text{fire}}) + S_i \tag{2}$$

where V_i represents the transmembrane potential of cell i, τ its membrane time constant, V_0 its resting potential and S_i the external stimulus. Here $k_{ij}(t)$ is a binary random variable which is one with probability p, and is zero otherwise. The parameter p is termed the synaptic reliability. Cell j fires when its potential reaches its firing threshold θ_j; afterwards its potential is reset to the resting value. The network is pulse coupled without delay through the delta function term, where t_j^{fire} labels the times when cell j fires. Coupling between cell i and j is given by J_{ij}. A dimensionless form of equation (2) is used where time and potentials are measured in terms of membrane time constant and threshold potential scales respectively:

$$\dot{v}_i = -v_i + \sum_j J_{ij} k_{ij}(t) \delta(t - t_j^{\text{fire}}) + s_i. \tag{3}$$

In this form the resting potential is subsumed within the stimulus, and the resting threshold value is normalized to 1. Thus the dimensionless stimulus term reflects both the post-firing reset level as well as the actual stimulus.

The firing threshold is dynamic to account for the increase in the threshold immediately after a neuron fires, and the gradual post-firing after-hyperpolarization. When a cell fires, its threshold increases by Δ_θ, then exponentially asymptotes to the resting threshold, $\theta = 1$:

$$\dot{\theta}_i = -\theta_i + \Delta_\theta \delta(t - t_i^{\text{fire}}) + 1. \tag{4}$$

Here, the threshold decay time constant is taken to be equal to the membrane time constant in order to retain analyticity in the time evolution of the model.

The network of cells is given a one-dimensional circular topology through the coupling, which is of the Mexican-hat form:

$$J_{ij} = a \exp\left(-\frac{d_{ij}^2}{2l_1^2}\right) - b \exp\left(-\frac{d_{ij}^2}{2l_2^2}\right) - c \qquad \text{for } i \neq j. \tag{5}$$

Here, d_{ij} is the shortest distance between units i and j on the circle. The parameters l_1 and l_2 determine the short-range excitation and medium-range inhibition length scales respectively. No self-coupling was allowed.

2.2. *Network of McGregor neurons*

In addition to the integrate-and-fire neuron model, we also simulated a network of McGregor neurons (McGregor and Oliver 1974). Their dynamics has some features of the Hodgkin–Huxley model and can be written as

$$\begin{aligned}\tau_E \cdot \dot{E}_i(t) = & -(E_i(t) - E^0) - (g_i(t) - g^0) \cdot (E_i(t) - E^K) \\ & - (E_i(t) - E^{ex}) \cdot \left[S \cdot s_i + \sum_j J_{ij}^{ex} \cdot o_j(t - \tau) \right] \\ & - (E_i(t) - E^{in}) \cdot \left[\sum_j J_{ij}^{in} \cdot o_j(t - \tau) \right] + \eta_i(t) \end{aligned} \tag{6}$$

$$\tau_\theta \cdot \dot{\theta}_i(t) = -(\theta_i(t) - \theta^0) + c \cdot E_i(t) \tag{7}$$

$$\tau_g \cdot \dot{g}_i(t) = -(g_i(t) - g^0) + \tau_g \cdot b \cdot o_i(t). \tag{8}$$

The variables E_i, θ_i and g_i describe the membrane potential, threshold recovery and potassium current of neuron i. E^K, E^{in}, E^{ex} denote the equilibrium values of E for the influence of potassium current, inhibitory input and excitatory input, respectively. $J_{ij}^{ex/in}$ denote the weights, τ the synaptic delay, S the smallest input necessary for repetitive firing, E^0, g^0 and θ^0 the equilibrium values of the respective variables, and $o_i(t)$ the spiking history of neuron i ($i = 1, \ldots, N$):

$$\begin{aligned} o_i(t) &= (\dot{E}_i - \dot{\theta}_i) \cdot \delta(E_i - \theta_i) && \text{for } \dot{E}_i > \dot{\theta}_i \\ o_i(t) &= 0 && \text{otherwise.} \end{aligned} \tag{9}$$

Throughout our simulations, $E^K = E^{in} = 1$, $E^{ex} = 7$, $E^0 = g^0 = 0$, $\theta^0 = 1$, $\tau_E = 2.5$ ms, $\tau_\theta = 10$ ms, $\tau_g = 1$ ms, $c = 0.3$, $\tau = 0.5$ ms, and $b = 4.0$. The synaptic weights are chosen similar to equation (5)

$$\begin{aligned} J_{ij}^{ex} &= a' \exp\left(-\frac{d_{ij}^2}{2l_1^2}\right) \\ J_{ij}^{in} &= b' \exp\left(-\frac{d_{ij}^2}{2l_2^2}\right) + c'. \end{aligned} \tag{10}$$

The McGregor neuron model is biologically more realistic than the integrate-and-fire model and can be simulated more quickly than a full Hodgkin–Huxley model. This model was used to test whether the phenomenon observed with integrate-and-fire models was generic.

3. Results

In a network of integrate-and-fire neurons, when the threshold recovery time constant is equal to the membrane time constant, the network evolution between successive spikes can be determined analytically. Given initial conditions and a constant Gaussian stimulus centred about a specific cell in the network, the time when the next cell fires is calculated and the network evolved to that instant in time. When a cell fires, its pulse is instantaneously transmitted to the other cells in the network, sometimes causing a cascade of cells to fire in synchrony. Two variants of the model arise, depending on how the avalanches of spike

activities are handled. In the first form, the time scale of cell reset is greater than the avalanche time scale. Consequently, all the cells that fire in the cascade of activity are effectively reset at the same time. In the second form, cells reset on a time scale shorter than or comparable to the coupling time scale (delays). In this version, cells that fire first are quickly reset to zero, and receive coupling from the subsequent cells that fire in the cascade. For this paper, we present results for the second variant, though many of the properties apply to both models. The mechanism of avalanche synchronization has been analysed elsewhere. (Hopfield and Herz 1995, Gerstner 1996, Herz and Hopfield 1995).

3.1. Clusters of elevated activity

When the units are uniformly distributed on a circle, all cells are equivalent and the network possesses a discrete translational symmetry. Consequently, the network has an attractor of the dynamics centred about every unit. Following Tsodyks and Sejnowski (1995a), we studied networks where this symmetry was broken either by having the units randomly positioned on the circle, or by having a sinusoidal variation of the unit positions. The latter breaks the underlying translational symmetry of the lattice, but retains a weaker 'cluster lattice' symmetry. This symmetry breaking, which could be due to underlying inhomogeneities or plasticity of the synapses, gives rise to discrete localized attractors (figure 1). Within these attractors, the cells fire at a higher firing rate.

The clustering of activity for the integrate-and-fire model and for the corresponding mean-field model described by equation (1) was similar, as shown in figures 1(*b*) and 1(*c*). In figure 1(*d*) the profile of the activity clusters is overlayed with the total sum of synaptic couplings to each neuron. The activity in the clusters tended to be all-or-none. In contrast to analytic studies of pulse coupled network models where the total sum of synaptic couplings to each neuron is normalized (Hopfield and Herz 1995, Gerstner 1996), our results suggest that variations in the total coupling to each neuron are important for the clustering of activity.

3.2. Temporal correlations and ISI variability

The integrate-and-fire model allows for the study of detailed spatial and temporal patterns of spiking activity. As mentioned before, cells in the attractor most strongly stimulated fire at the highest firing rates. However, as shown in figure 2(*a*), there is also a strong tendency for cells within a cluster to fire in synchrony. Furthermore, there is also synchronized activity at a low firing rate in neurons belonging to all the other attractors.

The synchronization property is robust to stochastic synaptic failure. With the synaptic reliability at 10%, coherent synchronization of firing within attractors is still strong. In addition, the coefficient of variation (CV) of the interspike intervals of the network resembles that of a Poisson process (CV = 1)† which often occurs for cortical neurons *in vivo*. In figure 3 a scatterplot of CV versus mean interspike interval is plotted. The consistently high coefficient of variation for the cells in the network (figure 2), as well as its variation with mean interspike interval (figure 3) is similar to data from visual cortex analysed by Softky and Koch (1993).

3.3. Persistence and rapid switching

By varying the coupling strength, threshold recovery and synaptic reliability parameters, the network exhibited a tendency for either persistence of activity within a cluster, or rapid

† CV is defined to be the variance divided by the mean of a distribution.

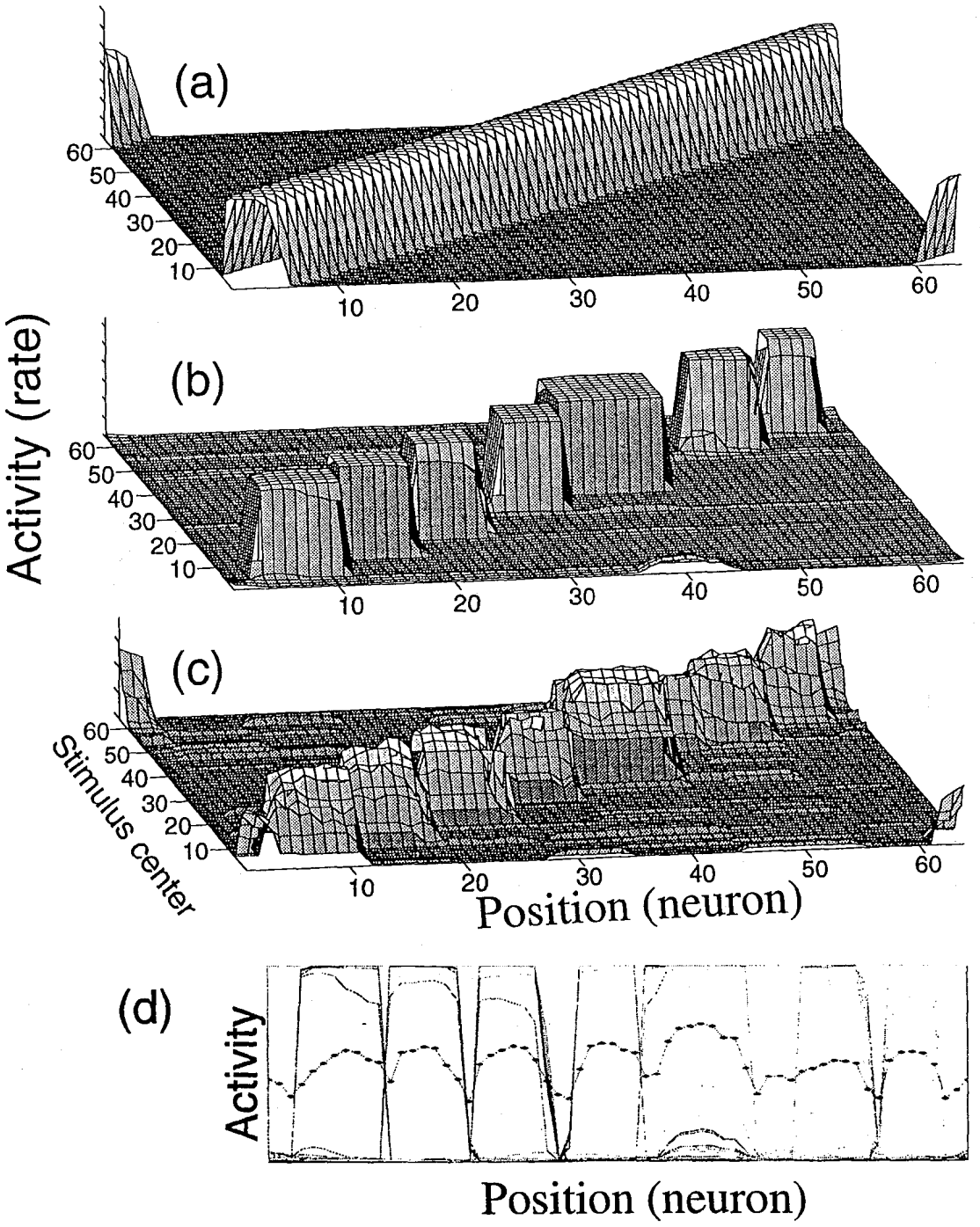

Figure 1. Symmetry breaking in the pattern of connectivity in a ring of neurons leads to clustering of activity. (*a*) Plot of cell activity for a mean-field model as a function of cell position and stimulus position for a translationally invariant network. The length scales in the Mexican hat coupling are $l_1 = 0.02$, $l_2 = 0.04$. (*b*) Activity plot for a mean-field model in a non-translationally invariant network. Coupling corresponded to cells randomly distributed around the circle with the same Mexican-hat coupling length scales. (*c*) The activity plot for an integrate-and-fire network with the same coupling matrix as in (*b*). All activities are in arbitrary dimensionless units. (*d*) Plot of the activities for all the cells for all stimuli positions in (*c*), showing profiles of the localized attractors (dotted lines). The total synaptic coupling to each cell is superimposed using diamond points in arbitrary units.

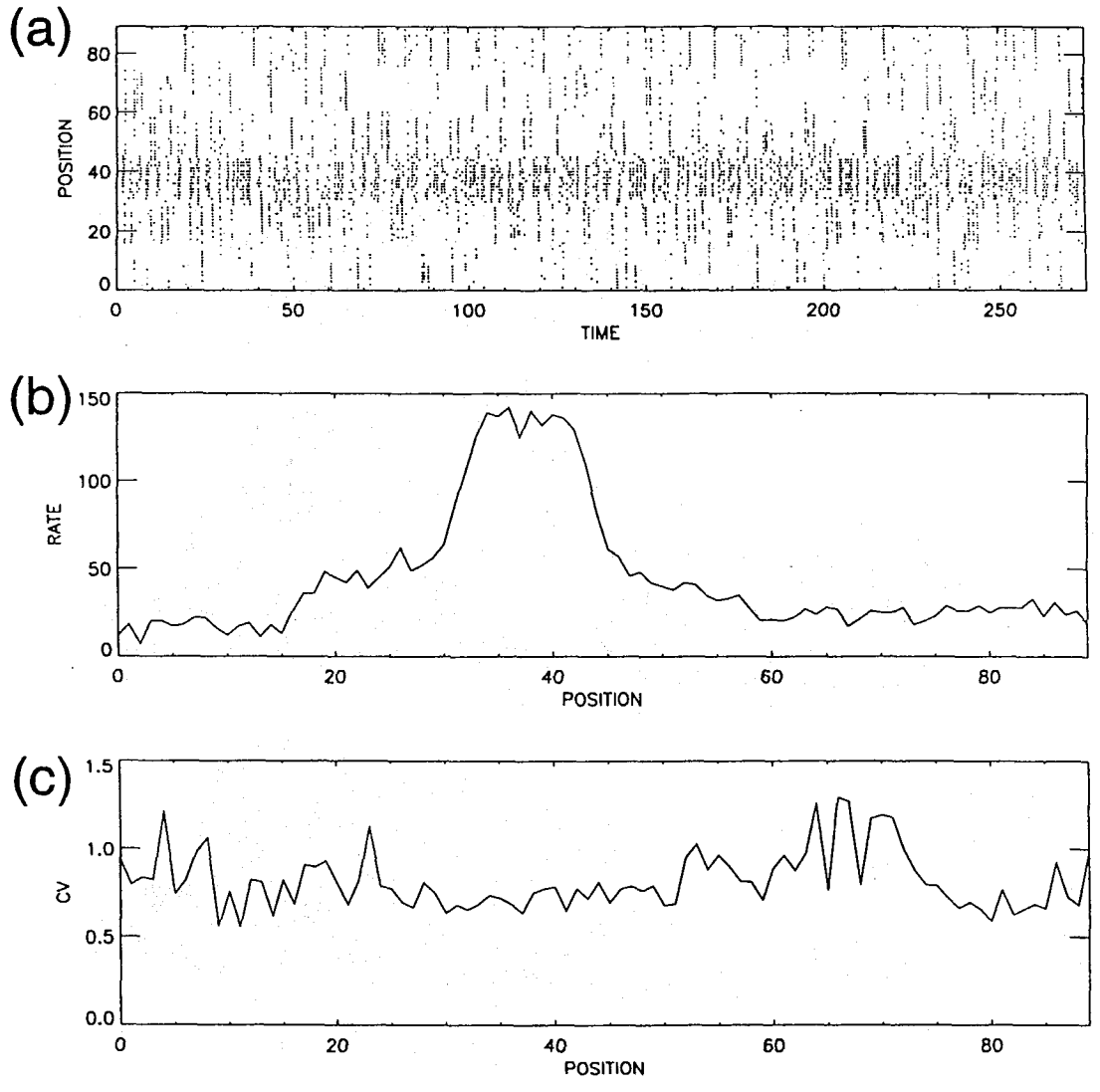

Figure 2. Firing pattern for artificially constructed network of 90 cells with six equivalent attractors. (*a*) Raster plot of spiking neurons where each point corresponds to a spike. (*b*) Firing rate profile in dimensionless units. (*c*) CV of the interspike interval of each cell. Locations of the cells are sinusoidally modulated with an amplitude of 2/90. The Mexican hat coupling was: $l_1 = 0.04$, $l_2 = 0.2$, $a = 3$, $b = 0.672$, $c = 0$. Stimulus was chosen to be a Gaussian of amplitude 0.2 and width 7/90, offset by 1.01, centred at cell number 38; thus all cells receive supra-threshold stimulus. Initially, the voltages of all the cells were randomly distributed between 0 and 1.

switching of activity from one cluster to another, as shown in figure 4 (see also Tsodyks and Sejnowski 1995b).

For the purpose of analysis, consider a simplified symmetric coupling given by constant excitation within a cluster of strength a and a uniform inhibition of strength c. First, assume mean field excitatory and inhibitory coupling where the stochastic element is averaged out. This results in a deterministic excitatory coupling within clusters of strength pa and uniform inhibitory coupling of strength pc. Here p is the synaptic reliability. A slight variation of the initial voltages in a network with nearly uniform supra-threshold stimulus could cause

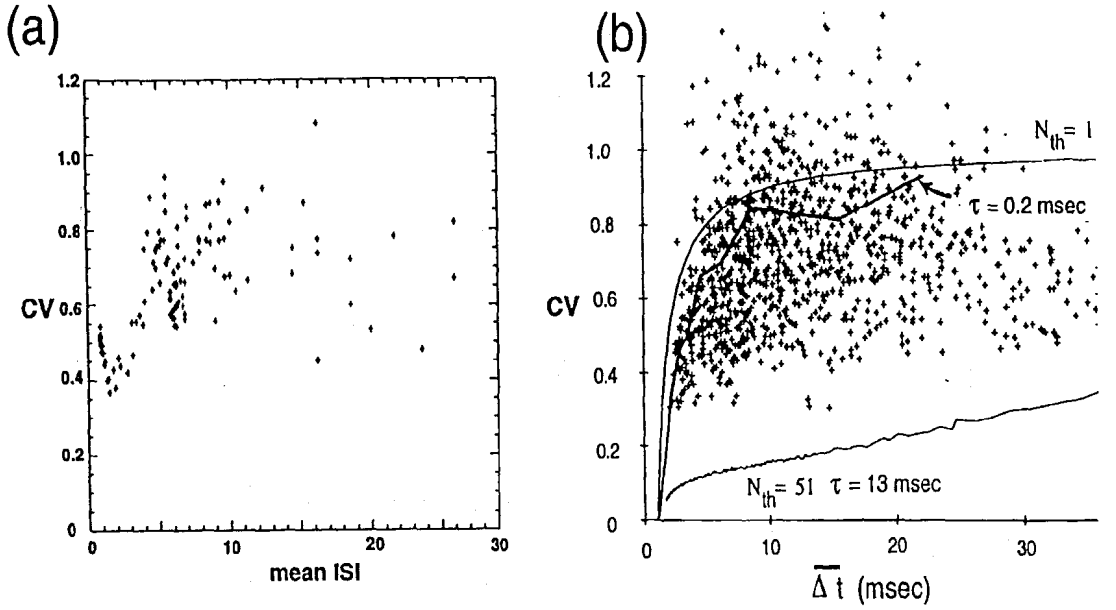

Figure 3. Scatterplots of CV versus mean interspike interval. (*a*) Plot of CV versus mean interspike interval (ISI) for cells firing more than 10 times in the simulation. Cells firing at a high rate tend to have lower CV. The network consisted of 180 cells with six equivalent attractors; the parameters $\Delta_\Theta = 0$, $a = 0.4$, $c = 0.088$ and $p = 0.1$ were used. (*b*) Similar plot reproduced (with permission) from Softky and Koch (1993) of the coefficient of variation for macaque cortical neurons. For details, please refer to Softky and Koch (1993).

firing of one specific attractor with n cells to persist indefinitely if (see the appendix for details):

$$p(a(n-1)+c) - 1 - \Delta_\Theta > 0. \tag{11}$$

Infinite persistence will not hold with stochastic elements in the couplings. When only the stochastic element in the inhibitory coupling is averaged out, the expected persistence length of the clustered synchronous activity can be approximated as shown in the appendix. In this calculation, the external stimulus is not assumed to be uniform so that coupling driven persistence of activity can be contrasted with stimulus driven switching of activity. The expected persistence length, measured by the number of cooperative cascades of activity in a cluster is given by (see the appendix for details):

$$\langle l \rangle = \frac{q}{1-q} \tag{12}$$

where

$$q \approx \frac{1}{2}\left[1 + \operatorname{erf}\left(\frac{np - m}{\sqrt{2np(1-p)}}\right)\right] \tag{13}$$

is the probability of sustained activity of the cluster, and

$$m = \frac{1 + \Delta_\Theta}{p\left(a + c(s_j - s_k)/(s_k - 1)\right)} > 0 \tag{14}$$

is the critical number of cells in the cluster which has to fire in order to sustain the persistent activity.

These results show that the persistence of activity increases with higher synaptic reliability (p), stronger synaptic coupling (a, c), and smaller threshold adaptation (Δ_Θ).

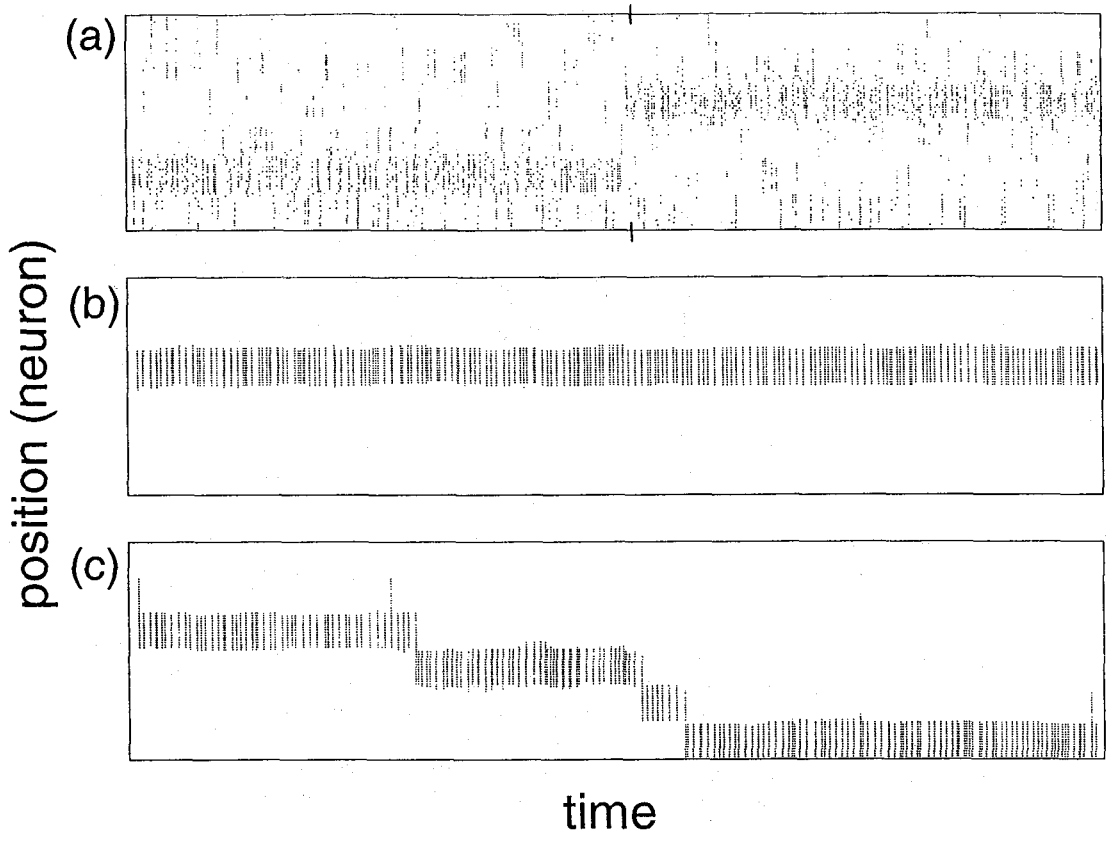

Figure 4. Rapid switching and persistence in the network. (*a*) Raster plot of spiking neurons. At the time indicated by the tickmarks, a stimulus identical to that used in figure 2 was shifted from one cluster centre to another. (*b*) Persistence of activity in the firing pattern. Stimulus was uniformly set to 1.01, $a = 1$, $b = 0.16$, $c = 0.08$, $p = 0.6$. $\Delta_\Theta = 0.1$. (*c*) A different time scale for persistence with the same stimulus but with $a = 0.8$, $b = 0.128$, $c = 0.064$, $p = 0.5$.

Although this calculation is only qualitatively correct, equations (12)–(14) successfully capture the effects of the parameters on persistence length, and give a rough lower bound on the switching time of the network.

4. More realistic simulations

Are the main results of elevated activity within a cluster, strong temporal correlation of clustered cells, and high CV in the interspike intervals robust? Do they remain valid in biologically more realistic models? In the strong coupling regime, the firing of a cell causes a cascade of cooperative activity amongst the cells with which it is strongly coupled. With more detailed models, instead of exact synchronization of firing times, as reflected in a sharp peak in the cross correlation of units within a cluster, a finite width should be observed. The results of the same stimulation paradigm as in figure 2, but using the McGregor neuron model (McGregor and Oliver 1974) are shown in figure 5. Neurons in the same cluster tend to fire synchronously, but due to the finite synaptic delay, synchronization takes place in waves propagating in the network. The autocorrelation of the summed activity from ten neurons within one cluster shows a sharp central peak, signaling a high degree of synchronization. In contrast, the cross-correlation between two clusters is flat (figure 5(*c*)).

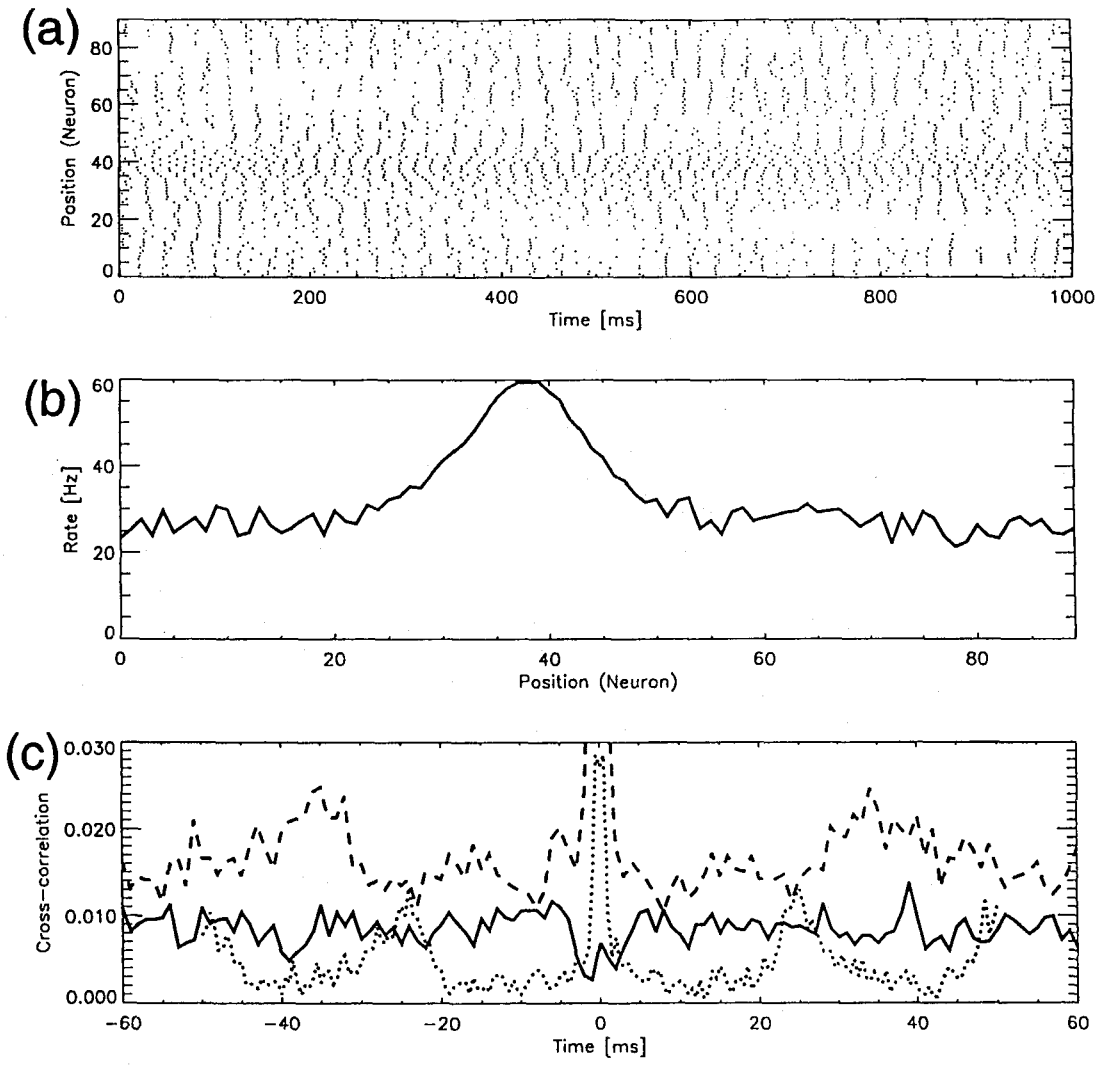

Figure 5. Robustness of clustered activity for the McGregor model compared with an integrate-and-fire model of the same network as in figure 2. Parameters are $a' = 0.9$, $b' = 1.0$, $c' = 1.0$, and $S \approx 0.2564$. (*a*) Raster plot of spiking neurons. (*b*) Firing rate profile. (*c*) Cross-correlograms of the summed activities from two sets of five different neurons in cluster 1 (dotted line), cluster 3 (dashed line), and clusters 1 and 3 (solid line). Cluster 1 contains neurons 1–15, and cluster 3 neurons 31–45. Note that the peak of the Gaussian input is centred on cluster 3, which has a higher average firing rate than cluster 1.

5. Discussion

A simple biologically motivated model was shown to exhibit surprisingly rich properties consistent with experimental findings in cerebral cortex. By varying the strength of the stimulus relative to the lateral coupling, the network can change from a stimulus-driven response where learning can take place, to a coupling-driven clustering response where short-term memory and processing can occur. In particular, activity is localized to clustered attractors, as described previously (Tsodyks and Sejnowski 1995a), and synchronization of cells occurs within clusters with a high interspike interval variance reminiscent of a Poisson point process. Furthermore, depending on the parameters, the clustered activity can either

switch rapidly when the stimulus was switched (Tsodyks and Sejnowski 1995b) or persist. In contrast, in mean-field models activities drift slowly from one position of stimulation to the next (Ben-Yishai *et al* 1995). Simple variations of basic model parameters allow for the fine tuning of persistence and switching times, effectively allowing the network to either retain information or be poised for a rapid response. It is possible that feedback from higher cortical areas may play a role in modifying the pertinent parameters.

The clustered synchronized activity in the network is reminiscent of the synchronized oscillator clusters reported by Terman and Wang (1995), who speculated on their possible role in binding features represented by a cluster of neurons and segmentation between uncorrelated clusters. The correlated firing seen for oriented cells in cat visual cortex (Gray *et al* 1989) and the dependence of correlation between clusters of oriented cells on stimuli (Engel *et al* 1992) fit nicely within the current framework. Finally, our model demonstrates that local synchronization does not necessarily require oscillations, consistent with recordings from monkey visual cortex (Kreiter and Singer 1996) where oscillations are negligible while there is significant stimulus-dependent synchronization.

We believe that the basic properties of our simple model (synchrony within a cluster, asynchrony between clusters, and high interspike interval variability) are generic in the sense that they also occur in more detailed and realistic neuron models. We tested this with simulations based on the McGregor model (McGregor and Oliver 1974). These results demonstrate the importance of temporal structure both for explaining a range of experimental findings and for a theoretical analysis of spatially-organized neuronal networks.

Acknowledgments

We are grateful for discussions with Michail Tsodyks. KP was supported by a grant number Pa 569/1-1 from the DFG. TJS received support from the Howard Hughes Medical Institute.

Appendix. Persistence length calculations

In the following analysis, the coupling is taken to be stepwise constant with local excitation between cells within a cluster with strength a and uniform inhibition with strength c. More precisely, we have n neurons in each of n_c clusters that are defined by the coupling matrix $J_{ij} = (a - c)$ for $ln < i, j \leqslant (l + 1)n$ where $0 \leqslant l < n_c$, and $J_{ij} = -c$ otherwise. Since no self-coupling is allowed, $J_{ii} = 0$. This symmetrical coupling matrix is a straightforward simplification of the sinusoidally modulated coupling introduced in section 3. We restrict our analysis to the case where the stimulus level is suprathreshold but very close to threshold for all the cells. Under these conditions, the voltage distribution of the units in the network will be sharply peaked just below the firing threshold. Thus, cells are almost always close to firing. When a cell, labelled j, in the cluster of interest fires, all other cells are assumed to be close to the threshold: $v_k \approx 1$ for $k \neq j$, where 1 is the threshold. This assumption effectively decouples the dynamics of the system from much of its past history.

Calculation 1. Mean-field excitation of strength pa, and inhibition of strength pc.

Since the stochastic elements have been averaged out, the cluster either fires indefinitely (infinite persistence) or just once. We consider the persistence of activity of a cluster triggered by cell j in the cluster. Let Δt_j be the time to firing of cell j in the absence of coupling, and s_j be the external stimulus received by the cell. The firing of neuron j triggers all $n - 1$ other neurons in this cluster to fire. The membrane potential of cell j is

reset to 0, and is subsequently raised by an amount of $(n-1)p(a-c)$ due to the firing of the $n-1$ other cells in the cluster. Neurons outside this cluster receive only inhibitory coupling, resulting in the decrease of their near threshold membrane potentials by npc. Let k label a typical cell outside the active cluster. From the analytical solutions of equations (2) and (3) in the absence of coupling, we find that in order to satisfy $\Delta t_j < \Delta t_k$, the following equation must hold:

$$\frac{s_j - p(n-1)(a-c) + \Delta_\Theta}{s_j - 1} < \frac{s_k - (1-npc)}{s_k - 1}.$$

For $s_j \approx s_k$, we obtain

$$p(a(n-1)+c) - 1 - \Delta_\Theta > 0.$$

Calculation 2. Mean-field inhibition of strength pc, with stochastic excitatory coupling of strength a and reliability p.

There is a critical number of cells m in the 'active attractor' that must fire in order to sustain the activity of the attractor—to make cell j in the cluster be the next cell to fire after a cascade, and to cause the next cascade to be in the same cluster. To compute the critical value m, assume m of the cells in the cluster containing cell j fired, and solve $\Delta t_j = \Delta t_k$:

$$\frac{s_j - mp(a-c) + \Delta_\Theta}{s_j - 1} = \frac{s_k + mcp - 1}{s_k - 1}.$$

This gives

$$m = \frac{1 + \Delta_\Theta}{p\big(a + c(s_j - s_k)/(s_k - 1)\big)}.$$

The probability of sustained activity, q, is given by the probability that m or more cells in the active cluster fire, given stochastic excitatory coupling with probability p. This amounts to summing a few terms in a binomial distribution. The Gaussian approximation of the binomial distribution is used, with the sum approximated by the integral of the Gaussian distribution from m to n: ($n \gg 1$, $n(1-p) \gg 1$, $np(1-p) \gg 1$ and m is within a $\sqrt{np(1-p)}$ neighbourhood of np):

$$q = \sum_{i=m}^{n} \binom{n}{i} p^i (1-p)^{n-i} \approx \frac{1}{2}\left[1 + \operatorname{erf}\left(\frac{np - m}{\sqrt{2np(1-p)}}\right)\right].$$

Finally, the expected persistence length as measured in the number of cooperative cascades of activity in the cluster is given by

$$\langle l \rangle = \sum_l l q^l (1-q) = \frac{q}{1-q}.$$

For example, this shows that by increasing the external stimulus s_j to cell j relative to the stimulus to cell k in a competing cluster, the critical cluster activity number m decreases, and hence the persistence length of activity in the cluster containing cell j increases. Alternatively, increasing s_k relative to s_j reduces the persistence length and results in a faster switching to activity in in the cluster containing cell k.

References

Ben-Yishai R, Lev Bar-Or R, and Sompolinsky H 1995 Theory of orientation tuning in visual cortex *Proc. Natl Acad. Sci. USA* **92** 3844–8

Engel A K, König P, Kreiter A K, Schillen T B and Singer W 1992 Temporal coding in the visual cortex: new vistas on integration in the nervous system *Trends Neurosci.* **15** 218–26

Gerstner W 1996 Rapid phase locking in systems of pulse-coupled oscillators with delays *Phys. Rev. Lett.* **76** 1755–8

Gray C M, König P and Engel A K 1989 Oscillatory responses in cat visual cortex exhibit inter-columnar synchronization which reflects global stimulus properties *Nature* **338** 334–7

Herz A V and Hopfield J J 1995 Earthquake cycles and neural reverberations: collective oscillations in systems with pulse-coupled threshold elements *Phys. Rev. Lett.* **75** 1222–5

Hopfield J J and Herz A V 1995 Rapid local synchronization of action potentials: toward computation with coupled integrate-and-fire neurons *Proc. Natl Acad. Sci. USA* **92** 6655–62

Kreiter A and Singer W 1996 Stimulus dependent synchronization of neuronal responses in the visual cortex of the awake macaque monkey *J. Neurosci.* **16** 2381–96

Mainen Z F and Sejnowski T J 1995 Reliability of spike timing in neocortical neurons *Science* **268** 1503

McGregor R J and Oliver R M 1974 A model for repetitive firing in neurons *Kybernetik* **16** 53

Softky W R and Koch C 1993 The highly irregular firing of cortical cells is inconsistent with temporal integration of random EPSPs *J. Neuroscience* **13** 334–50

Terman D and Wang D 1995 Global competition and local cooperation in a network of neural oscillators *Physica* D **81** 148–76

Troyer T and Miller K 1997 Physiological gain leads to high ISI variability in a simple model of a cortical regular spiking cell *Neural Comput.* **9** 971–83

Tsodyks M and Sejnowski T 1995a Associative memory and hippocampal place cells *Int. J. Neural Syst.* **6** (Suppl.) 81–6

——1995b Rapid state switching in balanced cortical network models *Network: Comput: Neural Syst.* **6** 111–24

Vreeswijk C and Sompolinsky H 1996 Chaos in neuronal networks with balanced excitatory and inhibitory activity *Science* **274** 1724–6